Filament-Induced Surface Spiral Turbulence in Three-Dimensional Excitable Media

Jörn Davidsen,[1,*] Meng Zhan,[2,†] and Raymond Kapral[3,‡]

[1]Complexity Science Group, Department of Physics & Astronomy, University of Calgary, Calgary, Alberta T2N 1N4, Canada
[2]Wuhan Institute of Physics and Mathematics, The Chinese Academy of Sciences, Wuhan 430071, China
[3]Chemical Physics Theory Group, Department of Chemistry, University of Toronto, Toronto, Ontario M5S 3H6, Canada
(Received 16 April 2007; revised manuscript received 11 April 2008; published 11 November 2008)

Filament-induced surface defect-mediated turbulence in bounded three-dimensional (3D) excitable media is investigated in the regime of negative line tension. In this regime turbulence arises due to unstable filaments associated with scroll waves and is purely a 3D phenomenon. It is shown that the statistical properties of the turbulent defect dynamics can be used to distinguish surface defect-mediated turbulence from its 2D analog. Mechanisms for the creation and annihilation of surface defects are discussed and Markov rate equations are employed to model the results.

DOI: 10.1103/PhysRevLett.101.208302 PACS numbers: 82.40.Ck, 05.45.Xt, 47.54.−r

Spiral wave patterns in two-dimensional excitable and oscillatory media are organized around phase defects where the local phase of the oscillation is not defined. Turbulent states, where pairs of defects with opposite topological charge annihilate in collisions and new pairs of defects are continuously created, can exist in such systems. This defect-mediated turbulence has been investigated both in simulation and experiment and is believed to be important in processes such as cardiac fibrillation [1,2], electroconvection in liquid crystals [3], fluid convection [4,5], autocatalytic chemical reactions [6,7], and Langmuir circulation in the oceans [8].

While defect-mediated turbulence in 2D media—including the spiral breakup instabilities leading to it—is well understood [9–15], much less is known about its analog in 3D media where another mechanism for wave turbulence may operate: complex behavior in space and time can emerge from the disorderly dynamics of vortex filaments of scroll waves [16–20]. This purely 3D phenomenon arises from the negative-tension instability of vortex filaments, which causes filaments to stretch, bend, and loop. The end points of filaments on the surface are topological defects that exhibit dynamics (referred to here as surface defect-mediated turbulence) which is similar in many respects to 2D defect-mediated turbulence. Figure 1 shows the structure of the spiral waves on one face of the cube, which directly reflects the underlying scroll wave and filament structure in the 3D medium.

The relevance of this 3D mechanism for ventricular fibrillation is a matter of some controversy [1,17,21,22]. One reason for this is that usually only the surface of the 3D cardiac medium is accessible to experimental observation. In such experiments the full dynamics of the filaments cannot be monitored. By contrast, most numerical studies of excitable cardiac models have focused on the filament dynamics (see, e.g., Refs. [23] and references therein). These observations prompt the general question, is it possible to distinguish between the 3D mechanism for turbulence and the 2D spiral breakup mechanisms in physical, chemical, and biological systems if observations are confined to the dynamics of spiral waves on the surface?

In this Letter, we determine the statistical properties of turbulent states generated by the negative-tension instability of vortex filaments in excitable media. We show that it is sufficient to study the dynamics on the surface of the 3D medium in order to distinguish the 2D and 3D mechanisms. This allows us to make predictions which can be experimentally verified by observations of surface defect-mediated turbulence in 3D excitable media.

We consider a cubical 3D excitable medium with sides of length L and no-flux boundary conditions on its surface. The kinetics is described by Barkley's model [24]

$$\partial_t u = D_u \nabla^2 u + \frac{1}{\epsilon} u(1-u)\left(u - \frac{v+b}{a}\right), \qquad (1)$$
$$\partial_t v = D_v \nabla^2 v + u - v.$$

Here, $u(\mathbf{r}, t)$ and $v(\mathbf{r}, t)$ are the activator and the inhibitor fields, respectively. The parameters were chosen to be $\epsilon = 0.02$, $a = 1.1$, $b = 0.21$, $D_u = 1$, and $D_v = 0$. The coordinates of the filaments were determined from the intersections of the two isosurfaces $u_0 = \frac{1}{2}$ and $v_0 = a/2 - b$ [25]. For these parameters the medium is weakly excitable

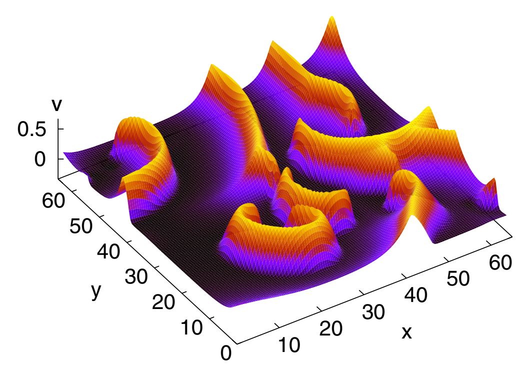

FIG. 1 (color online). Snapshot of the v field in the turbulent state on one of the surface sides of the cube. 11 spiral cores are visible which are the end points of the filaments.

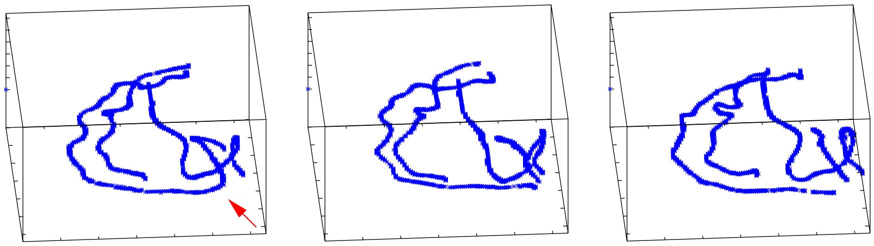

FIG. 2 (color online). Creation of a new filament. Initially, three filaments are present in the system. One of them (see arrow) collides with the boundary leading to the separation of the filament into two. A new surface defect pair is generated.

and well within the regime of negative line tension. Furthermore, under these conditions previous results [19,20] and our simulations have shown that the system is not turbulent in 2D and filaments rarely undergo fragmentation before they touch the boundaries [26]. This allows us to study filament turbulence in a simple context. The initial conditions were chosen to produce a scroll wave that subtends the volume. The model was integrated [27] for a sufficiently long time for a statistically stationary state to be observed where the volume contains a fluctuating number of vortex filaments whose total length fluctuates about a constant average value. Since the mechanisms leading to 2D turbulence do not operate in the excitable medium considered here, if the last filament is annihilated in the course of the dynamics the system will relax to the stable steady state and turbulence will be extinguished. However, we have never observed an extinction of turbulence on the long time scale of our simulations [28].

In 2D systems, the essential statistical features of defect-mediated turbulence in both experiments and simulations are captured by a simple Markov model which treats defect pairs as *statistically independent* entities. Gil *et al.* [10] assumed that defect pairs are created at a constant rate, $c(n) = c$, and annihilated at a rate proportional to the square of the number of defect pairs, $a(n) = an^2$, since defects can only annihilate in pairs of opposite topological charge. In this stochastic model the stationary probability distribution (PD) for the number of defect pairs is given by $p(n) = [c(n-1)/a(n)]p(n-1)$ whose solution is a squared Poissonian distribution $p(n) \propto (c/a)^n/(n!)^2$. Modifications to the rates must be made when boundary effects or noise have to be taken into account [5,7,29].

We adopt a similar approach to describe surface defect-mediated turbulence. The essential ingredients of the Markov model are the creation and annihilation rates. The mechanisms that lead to the creation and annihilation of surface defect pairs in the presence of the 3D negative-tension instability are fundamentally different from those in 2D. (1) Creation is due to filament collisions with the boundary. Such collisions break filaments into two segments forming a new surface pair of defects with opposite topological charge (see Fig. 2). If we assume the filaments to be statistically independent and, thus, uniformly distributed in the volume, it directly follows that the creation rate of surface defects should be proportional to the number of filaments—which is the same as the number of defect pairs for our model parameters—since the creation rate is determined by the growth rate of the filaments. Thus, $c(n) \propto n$. (2) The destruction of filaments and the accompanying annihilation of defect pairs occurs when small filament segments—generated in the creation process—shrink and disappear as shown in Fig. 3. For small segments with high curvature, the equations leading to the negative-tension instability [16,30], which were derived under the assumptions of linelike filaments and small curvature, no longer apply. In such cases filament segments can shrink instead of grow as shown in Fig. 3. In this process, the surface defects with opposite topological charge at the filament's end points collide and annihilate. While destruction mechanisms involving defects associated with different filaments are possible, these events do not play a detectable role in our simulations. Consequently, only a linked pair of defects can annihilate implying that the annihilation rate is proportional to the number of defect pairs and $a(n) \propto n$. This assumes statistically independent filaments.

The computed surface creation and annihilation rates as a function of the number of defect pairs for different L are presented in Fig. 4. For not too small L and n these rates can be fit by the forms

$$c(n) = \beta_1 + \beta_2 n, \qquad a(n) = \alpha_1 + \alpha_2 n. \tag{2}$$

Using these rates and solving for the stationary solution of the Markov model, instead of the squared Poissonian distribution of 2D turbulence, we find

$$p(n) = p(n_0)\frac{z^{n-n_0}\Gamma(n+z_1)\Gamma(n_0+z_2+1)}{\Gamma(n+z_2+1)\Gamma(n_0+z_1)}, \tag{3}$$

where $z_1 = \beta_1/\beta_2$, $z_2 = \alpha_1/\alpha_2$, $z = \beta_2/\alpha_2$, $n_0 \in \mathbb{N}$ and Γ the gamma function. This functional form is a direct consequence of the forms of the rates given in Eq. (2) and

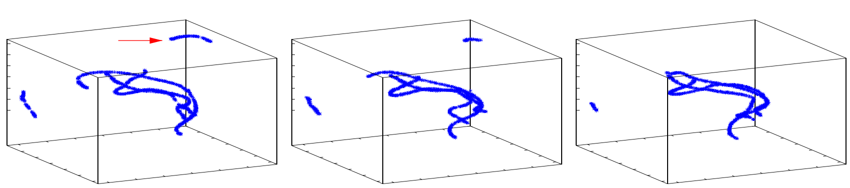

FIG. 3 (color online). Annihilation of filaments. Initially, five filaments are present. Two of them are short and well separated from the others.

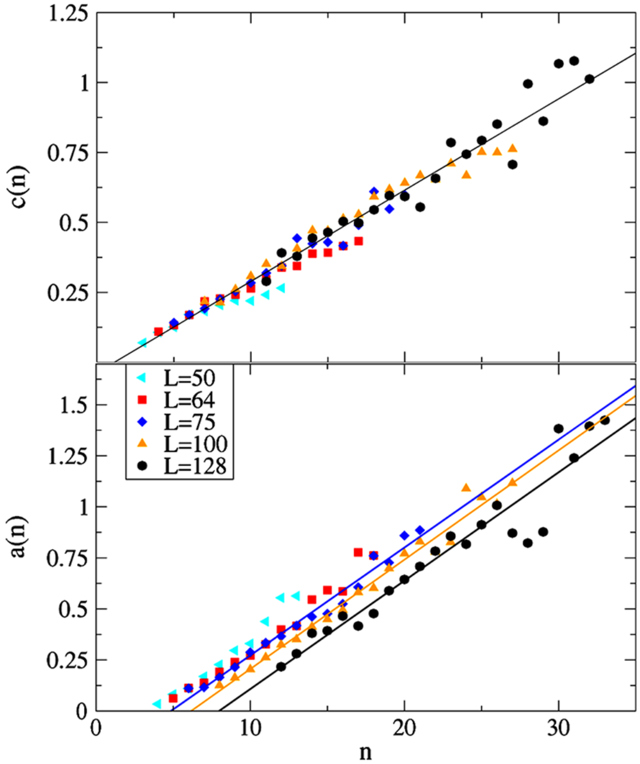

FIG. 4 (color online). Creation and annihilation rates as a function of the number of defect pairs for different L. Only data points with statistical errors less than 12% are shown [33]. Lines correspond to fits to those points according to Eqs. (2). We find $\beta_1 = -0.037 \pm 0.012$, $\beta_2 = 0.033 \pm 0.001$ for the creation rates. For the annihilation rates, we find $\alpha_{1,L=75} = -0.26$, $\alpha_{2,L=75} = 0.053$, $\alpha_{1,L=100} = -0.33$, $\alpha_{2,L=100} = 0.054$, $\alpha_{1,L=128} = -0.42$, $\alpha_{2,L=128} = 0.053$. Note the deviations from linear behavior for $L = 50$ in both cases.

n_0 represents the lowest value for which the latter is accurate. The predictions of Eq. (3) compare generally well with the measured value of $p(n)$ for large L as shown in Fig. 5 [31]. The forms of the creation and annihilation rates, as well as the form of the defect PD, are clearly different from those for 2D defect-mediated turbulence, even if boundary effects [5,7], noise [29], or strong correlations between defects [7] are included. The forms of these rates are the main signatures of filament-induced surface defect-mediated turbulence.

To evaluate the assumption of statistically independent filaments—which was necessary to predict linear creation and annihilation rates—and its failure for small L, we consider how the average surface density of defect pairs, $\rho_d = \langle n \rangle/(6L^2)$, and the average volume per total filament length $\langle V_f \rangle = L^3/\langle L_f \rangle$ vary with L. Figure 6 shows that ρ_d decays as $1/L$ while $\langle V_f \rangle$ grows as L. If filaments are uniformly distributed in the volume, this implies that filaments and associated defect pairs interact more strongly for small L explaining the breakdown of the assumption of statistically independent filaments.

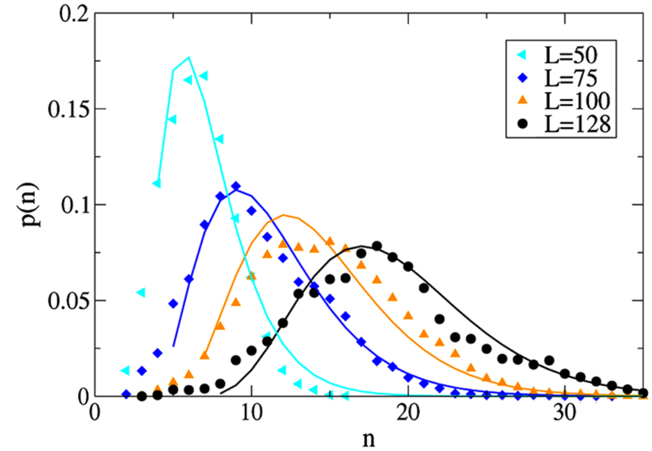

FIG. 5 (color online). Normalized histogram of the number of defect pairs for different L. The solid lines are the theoretical prediction [Eq. (3)] using the rates determined in Fig. 4.

However, correlations do exist even for large L: For very large system sizes, for a different excitable medium, the formation and persistence of *intermittently* stable triple filaments strands in large systems was observed [32]. Three nearby filaments with similar orientation form a triple-stranded bound state, effectively generating a three-armed scroll wave. Such transient bound states are also visible in Figs. 2 and 3 for our system. Since the formation of triple strands is accompanied by an increase in the excitation frequency, single filaments are pushed out of the system enhancing the destruction rate. This contribution to the annihilation rate should be independent of the number of filaments present in the system implying a positive constant term. Indeed, we find that the linear dependence of $a(n)$ breaks down for small n—independent of L—giving rise to a significantly higher (positive) annihilation rate (not shown). While the large statistical fluctuations do not allow us to verify the existence of a constant regime in $a(n)$, the observations are at least consistent.

Figure 7 gives further evidence for the effects of transient bound states. Since the formation of triple strands

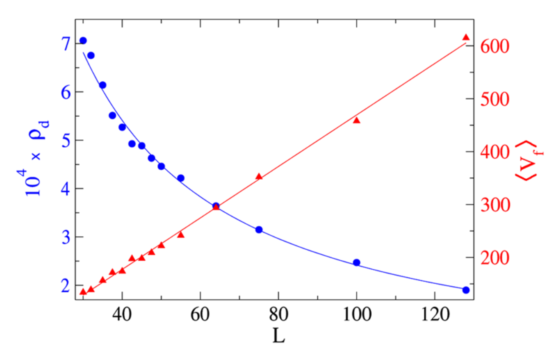

FIG. 6 (color online). Average surface density of defect pairs (blue circles) and average volume per filament (red triangles) as a function of system size. The lines correspond to a hyperbolic and a linear fit, respectively.

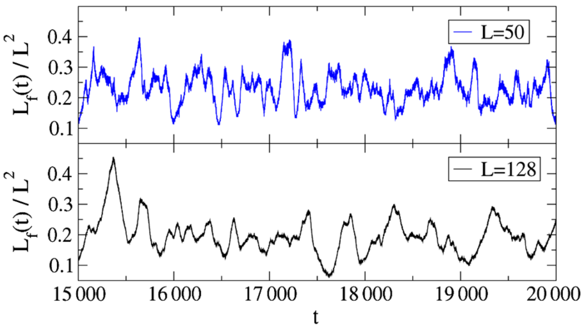

FIG. 7 (color online). Rescaled total filament length $L_f(t)$ as a function of time for different L.

pushes single filaments out of the system, it leads to a more regular, laminar state until the bound state breaks up. In Fig. 7, the turbulent dynamics shows incipient intermittency for large L. Yet, there are no well-defined laminar periods even for the largest L. This indicates that the lifetime of the bound states is rather short limiting the effect of the correlations due to intermittency.

We have shown that the statistical properties of surface defect-mediated turbulence allow us to distinguish between the mechanism for 3D filament-induced spiral turbulence and 2D spiral breakup mechanisms. In particular, for large systems, the appearance of the linear contribution to the creation rate allows one to make a clear distinction between the 2D and 3D mechanisms. Our results suggest that a statistical description of surface defects in systems with 3D spiral turbulence can provide useful insight into the dynamics. Even for more complex models than that considered here, such as those used in modeling cardiac fibrillation and chemical dynamics, the general ideas that underlie our statistical analysis of surface spiral turbulence should prove useful for understanding the mechanisms that control the turbulent behavior.

We would like to thank H. Chaté for helpful discussions. Research supported in part by NSERC, NNSFC (M. Z.), and Bairenjihua Foundation (M. Z.).

*davidsen@phas.ucalgary.ca
†zhanmeng@wipm.ac.cn
‡rkapral@chem.utoronto.ca

[1] F. H. Fenton, E. M. Cherry, H. M. Hastings, and S. J. Evans, Chaos **12**, 852 (2002).
[2] J. M. Davidenko, A. M. Pertsov, R. Salomonsz, W. Baxter, and J. Jalife, Nature (London) **355**, 349 (1992).
[3] I. Rehberg, S. Rasenat, and V. Steinberg, Phys. Rev. Lett. **62**, 756 (1989).
[4] A. L. Porta and C. M. Surko, Physica (Amsterdam) **139D**, 177 (2000).
[5] K. E. Daniels and E. Bodenschatz, Phys. Rev. Lett. **88**, 034501 (2002).
[6] Q. Ouyang and J. M. Flesselles, Nature (London) **379**, 143 (1996).
[7] C. Beta, A. S. Mikhailov, H. H. Rotermund, and G. Ertl, Europhys. Lett. **75**, 868 (2006).
[8] T. M. Haeusser and S. Leibovich, Phys. Rev. Lett. **79**, 329 (1997).
[9] P. Coullet, L. Gil, and J. Lega, Phys. Rev. Lett. **62**, 1619 (1989).
[10] L. Gil, J. Lega, and J. L. Meunier, Phys. Rev. A **41**, 1138 (1990).
[11] M. Hildebrand, M. Bär, and M. Eiswirth, Phys. Rev. Lett. **75**, 1503 (1995).
[12] G. D. Granzow and H. Riecke, Phys. Rev. Lett. **87**, 174502 (2001).
[13] J. Davidsen and R. Kapral, Phys. Rev. Lett. **91**, 058303 (2003).
[14] M. Bär and L. Brusch, New J. Phys. **6**, 5 (2004).
[15] I. S. Aranson and L. Kramer, Rev. Mod. Phys. **74**, 99 (2002).
[16] P. K. Brazhnik, V. A. Davydov, V. S. Zykov, and A. S. Mikhailov, Sov. Phys. JETP **66**, 984 (1987).
[17] A. T. Winfree, Science **266**, 1003 (1994).
[18] V. N. Biktashev, A. V. Holden, and H. Zhang, Phil. Trans. R. Soc. A **347**, 611 (1994); V. N. Biktashev, Int. J. Bifurcation Chaos Appl. Sci. Eng. **8**, 677 (1998); T. Bánsági and O. Steinbock, Phys. Rev. E **76**, 045202(R) (2007); C. Luengviriya, U. Storb, G. Lindner, S. C. Müller, M. Bär, and M. J. B. Hauser, Phys. Rev. Lett. **100**, 148302 (2008).
[19] H. Henry and V. Hakim, Phys. Rev. Lett. **85**, 5328 (2000); Phys. Rev. E **65**, 046235 (2002).
[20] S. Alonso, F. Sagués, and A. S. Mikhailov, Science **299**, 1722 (2003); S. Alonso, R. Kähler, A. S. Mikhailov, and F. Sagués, Phys. Rev. E **70**, 056201 (2004).
[21] R. A. Gray, J. Jalife, A. V. Panfilov, W. T. Baxter, C. Cabo, J. M. Davidenko, A. M. Pertsov, P. Hogeweg, and A. T. Winfree, Science **270**, 1222 (1995).
[22] S. Alonso and A. V. Panfilov, Chaos **17**, 015102 (2007).
[23] R. H. Clayton and A. V. Holden, IEEE Trans. Biomed. Eng. **51**, 28 (2004); R. H. Clayton, E. A. Zhuchkova, and A. V. Panfilov, Prog. Biophys. Molec. Biol. **90**, 378 (2006); A. V. Panfilov, Phys. Rev. E **59**, R6251 (1999).
[24] D. Barkley, M. Kness, and L. S. Tuckerman, Phys. Rev. A **42**, 2489 (1990).
[25] The positions of the filament end points on the surface were determined by computing topological charges [13].
[26] For other models under more general excitability conditions, including more realistic cardiac models [23], filaments may fragment in the interior of the system, sometimes producing scroll rings.
[27] The integration was performed using an Euler scheme with $\Delta t = 0.01$ and a 7-point Laplacian with $\Delta x = 0.5$.
[28] Depending on L, the lengths of the simulations were between 4000 and 10 000 spiral rotations.
[29] H. Wang, Phys. Rev. Lett. **93**, 154101 (2004).
[30] J. P. Keener, Physica (Amsterdam) **31D**, 269 (1988).
[31] In particular n_0 has to be large enough such that the fitted rates are physically reasonable, i.e., $a(n) > 0$ and $c(n-1) > 0$ for $n > n_0$.
[32] R. M. Zaritski, S. F. Mironov, and A. M. Pertsov, Phys. Rev. Lett. **92**, 168302 (2004).
[33] Note that the statistics collected for other points is insufficient to reliably estimate the rates.